THREE-DIMENSIONAL NONLINEAR DEGRADING MODEL FOR EARTHQUAKE RESPONSE ANALYSES OF CONCRETE BRIDGES

V. Phung[1] and D. Lau[2]

[1] *Structural Engineer, TranTech Engineering, Bellevue, WA, USA*
[2] *Professor, Dept. of Civil Engineering, Carleton University, Ottawa, ON, Canada*
Email: vphung@trantecheng.com, dtl@ccs.carleton.ca

ABSTRACT:
This paper presents a three-dimensional nonlinear degrading stiffness model capable of capturing stiffness degradation in bilateral directions for earthquake response analyses of reinforced concrete bridges. Stiffness degradations due to flexural and shear damage are considered. The model can trace the progress of damage from initial failure through gradual degradation of the member stiffness due to accumulative effects of damage to ultimate collapse. Flexural degradation is quantified by a cumulative flexural damage index, which is computed based on consideration of the maximum rotation and dissipated hysteretic energy of the element. Shear degradation is quantified by a shear damage index, which is derived from the shear demand and capacity relationship. Nonlinear earthquake response analyses of three-span reinforced concrete bridges subjected to bidirectional earthquake excitations are carried out to validate the model. Bridges of ductile dominated and shear dominated behavior structures are studied. Numerical results are presented in terms of the maximum displacement of bridge deck, moment at plastic hinges, local and global damage index and normalized hysteretic energy.

KEYWORDS:
Ground motion, earthquake response, damage index, shear degradation, non-linear analysis

1. INTRODUCTION

In the past three decades, there have been a number of studies on the development of three-dimensional nonlinear beam-column elements for modeling the inelastic plastic hinging behavior of reinforced concrete columns (Takeda et al. 1974, Tseng et al. 1973, Chen et al. 1982, Zhang et al. 1999, Phung 2005, etc.). Takeda et al. (1970) have proposed a hysteretic model based on experiment results from cyclic loading of reinforced concrete columns. Tseng and Penzien (1973) have developed a 3D elasto-plastic flexural column model for earthquake response analyses of highway bridges. Chen and Powell (1982) have developed a generalized 3D beam-column element, which considers the interaction of bending moment and axial force by means of yield interaction surface. The element has an elastic element and 2 hinges at the element ends to model the plastic behavior of the member. The stiffness of the plastic hinge is allowed to degrade when the member is subjected to loading reversal. The degradation of the stiffness is modeled as inverse proportioned to the largest previous hinge deformation. Zhang et al. (1999) have incorporated the degrading stiffness into the Tseng's model. In most previous studies, the stiffness degradation behavior of bridge column members is considered only related to flexural behavior.

Shear strength of bridge columns is separately assessed. Recent studies have shown that the shear strength of reinforced concrete columns at plastic hinge regions can be significantly reduced when the displacement ductility of the member increases (Wong 1993, Priestley 1994, etc.). The significant shear degradation in the plastic hinge region of columns is commonly observed in bridges designed prior to the 1970s. The reasons are due to insufficient transverse reinforcing steel, inadequate detailing and less conservative design requirements for shear strength compared to flexural strength. The interaction effect between the shear and flexural behavior of reinforced concrete columns can significantly affect their seismic responses and thus should be considered in the analysis model. The objective of this present study is to develop a three-dimensional nonlinear degrading stiffness model for seismic response analysis of reinforced concrete bridge columns that comprehensively takes into account the accumulated damage and the interdependency between flexural and shear mechanisms on the inelastic degradation behavior of reinforced concrete structural members. Earthquake response analyses of three-span reinforced concrete bridges subjected to bidirectional strong earthquake ground motions are carried out to illustrate the capabilities of the proposed model. Bridge column design and detailing with different amount of transverse reinforcing steel to represent typical bridge design of new and old bridge structures, of which the behavior are dominated by ductile flexural behavior or brittle shear behavior, respectively are considered.

2. POST-ELASTIC DAMAGE MEASURES

Post-elastic damage measures can be categorized as local and global damage measures. Both local and global damage measures are calibrated such that a value of zero indicates no damage while a value of one means total damage.

2.1. Local Damage Measures

2.1.1 Flexural damage index

During earthquakes, a reinforced concrete member may be damaged by the combined effect of loading amplitude and the number of loading cycles. To quantify the extent of damage in concrete structures subjected to severe earthquake excitations, the concept of damage index has been developed. A comprehensive review of different damage index models has been presented by William et al. (1995). For damage localized at the section ends of an element, Kunnath et al. (1992) have modified the Park and Ang's model (1985) as follows:

$$FD = \frac{\theta_{max} - \theta_y}{\theta_u - \theta_y} + \frac{\beta}{M_y \theta_u}\int dE_h \tag{2.1}$$

where θ_{max} is the maximum rotation angle sustained during loading history, θ_y is the yield rotation angle, and θ_u is the ultimate rotation capacity of the section, and M_y is the yield moment.

2.1.2 Normalized hysteretic energy

Normalized hysteretic energy (NHE) is adopted as the ratio of the hysteretic energy dissipated through cyclic response of the member normalized to twice the yield strain energy as follows:

$$NHE = \frac{\int dE_h}{M_y \theta_y} \tag{2.2}$$

2.1.3 Shear damage index

To evaluate the shear strength degradation of bridge columns it is more convenient to use member curvature ductility than displacement ductility. Displacement ductility can be related to curvature ductility as follows:

$$\mu_\Delta = 1 + 3(\mu_\phi - 1)\frac{L_p}{L}\left(1 - 0.5\frac{L_p}{L}\right) \tag{2.3}$$

where μ_Δ and μ_ϕ are the displacement and curvature ductility, respectively, L_p is plastic hinge length and L is column height. Figure 1 illustrates the shear behavior of three types of bridge columns. From the shear demand and shear capacity curves shown in Figure 1, the ultimate displacement ductility of a concrete member of case B can be computed as follows:

$$\mu_u = \begin{cases} < 1 & \text{Case A} \\ \mu_f - \dfrac{(\mu_f - \mu_i)(V_u - V_f)}{(V_i - V_f)} & \text{Case B} \\ \textit{Not applicable} & \text{Case C} \end{cases} \tag{2.4}$$

The computations of V_i and V_u follow the standard design procedure as presented in Priestley at al. (1996), to compute shear strength of reinforced concrete column considering shear contribution from concrete and reinforcing steel.

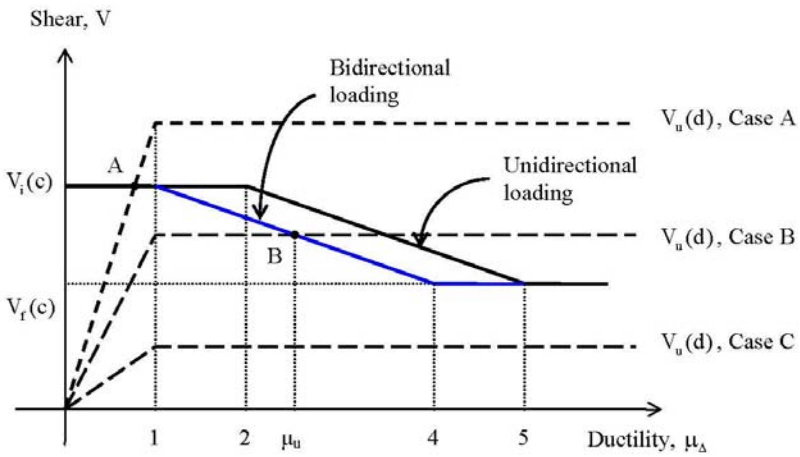

Figure 1 Shear Demand and Shear Capacity Relationship of Reinforced Concrete Columns.

For columns with plastic hinges, the shear demand is determined from the member moment capacity divided by the member length. A shear damage index is defined as a function of curvature ductility in this study as follows:

$$SD = \begin{cases} 0 & \text{if} \quad \mu_{max} < \mu_i \\ \dfrac{\mu_{max} - \mu_i}{\mu_u - \mu_i} & \text{if} \quad \mu_i \le \mu_{max} \le \mu_u \\ 1 & \text{if} \quad \mu_{max} > \mu_u \end{cases} \tag{2.5}$$

where μ_{max}, μ_i and μ_u are the maximum curvature ductility experienced during previous cycles, the curvature ductility where shear strength begins to degrade, and the ultimate curvature ductility, respectively.

2.2. Global Damage Measures

2.2.1 Global flexural damage index

The global flexural damage index is defined as the weighted sum of the local flexural damage indices of all structural members.

$$GFD = \sum_{i=1}^{N} w_i FD_i \tag{2.6}$$

$$w_i = \frac{HE_i}{\sum_{i=1}^{N} HE_i} \tag{2.7}$$

where w_i and HE_i are the weighting factor and dissipated hysteretic energy of the i-th damage member, respectively.

2.2.2 Global normalized hysteretic energy

The global normalized hysteretic energy is defined as the average of the normalized hysteretic energies absorbed by all members that experienced inelastic action, i.e.:

$$GHE = \frac{1}{N} \sum_{i=1}^{N} NHE_i \tag{2.8}$$

where N is the number of plastic hinges formed where seismic energy is dissipated.

2.2.3 Global shear damage index

The global shear damage index is also defined as weighted sum of the local shear damage indices of all the structural members as follows:

$$GSD = \frac{\sum_{i=1}^{N} SDI_i^2}{\sum_{i=1}^{N} SDI_i} \tag{2.9}$$

2. THREE-DIMENSIONAL NONLINEAR DEGRADING MODEL

This section presents the development of the three-dimensional degrading stiffness model for earthquake response analyses of three-dimensional structures. The degrading stiffness model is incorporated in an available beam-column element consisting of an elastic element and two zero-length plastic elements located at the two ends of the element (Tseng et al. 1973). The derivation of the degrading stiffness is described as follows. During elastic loading and unloading responses, the stiffness properties of a beam-column element are the elastic stiffness of the member. After yielding, the reloading stiffness in the opposite direction is degraded to reflect the damage effect on the load resistant behavior of the member. The degrading stiffness of a damaged element is modeled such that the degrading stiffness is between the stiffness of the undamaged state and that of fully damaged state. For illustration purposes the basic principle of the degrading model, the case of flexural damage about the z-direction and shear damage in the y-direction at one end of the member is described herein. Letting $\mathbf{k}_e$ be the stiffness matrix of the undamaged element with fixed-end condition as shown in Fig. 2a, $\mathbf{k}_{mz}$ be the stiffness matrix of an element with complete flexural damage at one end (pinned-end condition) as shown in Fig. 2b, $\mathbf{k}_{sz}$ be the stiffness matrix of an element with complete shear damage at one end (guided-end condition) as shown in Fig. 2c, and $\mathbf{k}_{msz}$ be the stiffness matrix of an element with complete flexural and shear damage at one end (roller-end condition) as shown in Fig. 2d, the degrading stiffness of a partially damaged element due to both flexural and shear damage at one end is expressed as follows.

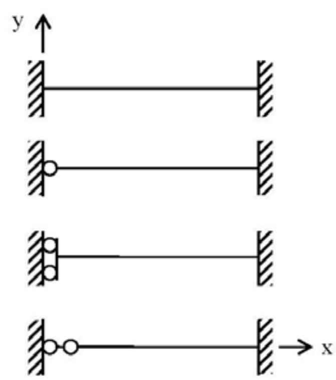

Figure 2 Damaged States at i-end: a) Undamaged State (FDI=0, SDI=0), b) Fully Damaged by Flexure (FDI=1), c) Fully Damaged by Shear (SDI=1), d) Fully Damaged by Both Flexure and Shear (FDI=1 and SDI=1).

$$\mathbf{k}_d = \mathbf{k}_e - FD\mathbf{k}_{dm} - SD\mathbf{k}_{ds} - (FD)(SD)\mathbf{k}_{dms} \tag{2.10}$$

In Eqn. 2.10, $\mathbf{k}_{dm}$ represents the maximum degrading effect of flexural damage on stiffness:

$$\mathbf{k}_{dm} = \mathbf{k}_e - \mathbf{k}_{mz} \tag{2.11}$$

The degrading effect of shear damage on the remaining stiffness is given by $\mathbf{k}_{ds}$. It is calculated as the difference between the remaining stiffness from flexural damage and the stiffness of fully damage condition by shear as follows:

$$\mathbf{k}_{ds} = \mathbf{k}_e - FD(\mathbf{k}_e - \mathbf{k}_{mz}) - \mathbf{k}_{sy} \tag{2.12}$$

For the case of combined flexural and shear damage as given by case B shown in Figure 1, the damage effect on the stiffness of the element is given by the difference between the remaining stiffness determined from Eqn. 2.11 and 2.12 and the stiffness of the fully damaged state by flexural and shear $\mathbf{k}_{dms}$ as follows:

$$\mathbf{k}_{\mathrm{dms}} = \mathbf{k}_{\mathrm{e}} - \mathrm{FD}(\mathbf{k}_{\mathrm{e}} - \mathbf{k}_{\mathrm{mz}}) - \mathrm{SD}\{\mathbf{k}_{\mathrm{e}} - \mathrm{FD}(\mathbf{k}_{\mathrm{e}} - \mathbf{k}_{\mathrm{mz}}) - \mathbf{k}_{\mathrm{sy}}\} - \mathbf{k}_{\mathrm{mzsy}} \tag{2.13}$$

The forms of $\mathbf{k}_{\mathrm{e}}$, $\mathbf{k}_{\mathrm{mz}}$, $\mathbf{k}_{\mathrm{sy}}$ and $\mathbf{k}_{\mathrm{mzsy}}$ can be found from Phung et al. (2005). Substituting Eqn. 2.11 to 2.13 into Eqn. 2.10, an alternative form of the degrading stiffness of a partially damage member due to both flexural and shear behavior at one end may be written as follows:

$$\begin{aligned} \mathbf{k}_{\mathrm{d}} = \mathbf{k}_{\mathrm{e}} &- \mathrm{SD}(\mathbf{k}_{\mathrm{e}} - \mathbf{k}_{\mathrm{ds}}) - \mathrm{FD}[\mathbf{k}_{\mathrm{e}} - \mathrm{SD}(\mathbf{k}_{\mathrm{e}} - \mathbf{k}_{\mathrm{ds}}) - \mathbf{k}_{\mathrm{m}}] \\ &- (\mathrm{SD})(\mathrm{FD})\{\mathbf{k}_{\mathrm{e}} - \mathrm{SD}(\mathbf{k}_{\mathrm{e}} - \mathbf{k}_{\mathrm{ds}}) - [\mathbf{k}_{\mathrm{e}} - \mathrm{SD}(\mathbf{k}_{\mathrm{e}} - \mathbf{k}_{\mathrm{ds}}) - \mathbf{k}_{\mathrm{m}}]\} \end{aligned} \tag{2.14}$$

The above derivation can be extended to the general case of damage at both or either ends of the member.

3. NUMERICAL EXAMPLES

3.1. Bridge Structure

A three-span concrete box girder bridge designed for an acceleration coefficient of 0.3 g is chosen for earthquake response analyses. Details of the bridge design can be found in the reference (FHWA 1996). Figure 3 shows the plan and elevation of the bridge.

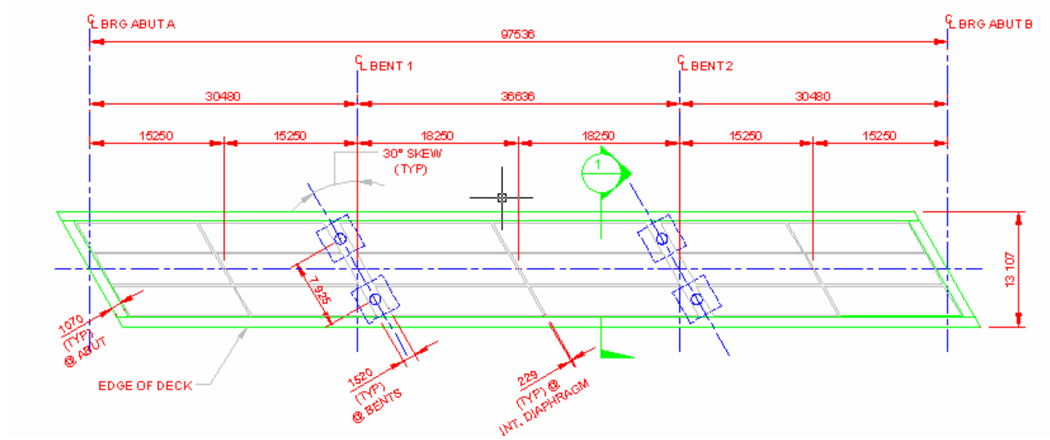

(a) Plan of the Bridge

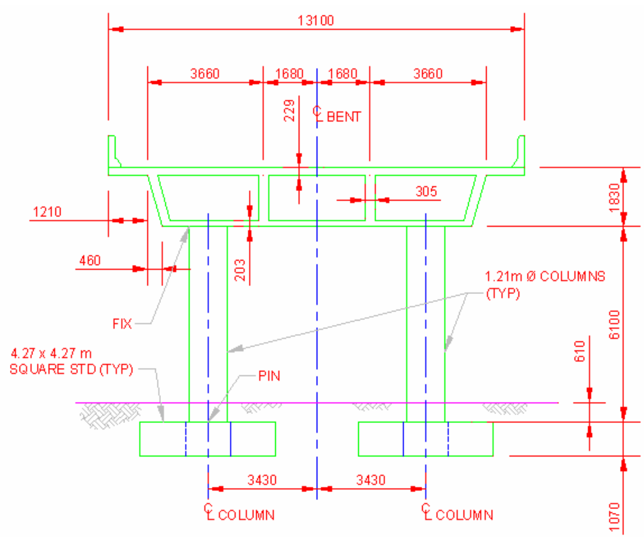

(b) Elevation

Figure 3 Plan and Elevation of the Bridge.

Three column types are examined in the present study: Bridge A (no flexural and no shear degradation), Bridge B (flexural degradation but no shear degradation), and Bridge C (both flexural and shear degradation).

Nonlinear earthquake response analysis of the example Bridges is performed using 16 sets of strong ground motions recorded from the 1971 Imperial Valley, the 1989 Loma Prieta, the 1994 Northridge and the 1999 Chi-Chi earthquakes. Table 3.1 lists the ground motion records selected from the PEER strong ground motion database (2006). These two components are then applied in the longitudinal and transversal directions of the Bridge with the larger magnitude component applied in the longitudinal direction.

Table 3.1 Ground Acceleration Dataset

Set	Event	Station	Distance (km)	Site class	PGA in x-dir (g)	PGA in y-dir (g)
C1	Chi-Chi, Taiwan	CHY088	42.82	C	0.216	0.144
C2	1999/09/20	ILA067	48.68	C	0.198	0.171
C3		TCU034	32.97	B	0.25	0.108
C4		TCU111	22.22	D	0.136	0.099
I1	Imperial Valley	Calexico Fire Station	10.6	D	0.275	0.202
I2	1979/10/15 23:16	El Centro Array #3	9.3	D	0.266	0.221
I3		EC County Center FF	7.6	D	0.235	0.213
I4		Holtville Post Office	7.5	D	0.253	0.221
L1	Loma Prieta	Coyote Lake Dam (Downstream)	22.3	D	0.179	0.16
L2	10/18/89 00:05	Gilroy Array #1	11.2	A	0.473	0.411
L3		Gilroy - Gavilan Coll.	11.6	B	0.357	0.325
L4		UCSC Lick Observatory	17.9	A	0.45	0.395
N1	Northridge	LA - Baldwin Hills	31.3	B	0.239	0.168
N2	01/17/94 12:31	Manhattan Beach - Manhattan	42.0	C	0.201	0.128
N3		La Crescenta - New York	22.3	C	0.178	0.159
N4		Stone Canyon	22.2	A	0.388	0.252

3.2. Numerical Results

Nonlinear earthquake response analyses of the Bridges A, B and C subjected to the selected earthquake ground motions are carried out. Numerical results are presented in terms of the maximum displacement, damage index and normalized hysteretic energy. The maximum displacement at the middle of the span 2 and bending moments at plastic hinges of columns are calculated. The damage behavior of Bridge columns during earthquake responses is traced by examining the evolution of the damage indices. The results demonstrate the validity and comprehensive capabilities of the proposed damage model.

To investigate the effects of degradation on seismic responses of Bridges A, B, and C, seismic response quantities are plotted against the peak ground acceleration. Figures 4a to 4d show the maximum displacement, flexural damage index, shear damage index, and normalized hysteretic energy of Bridges A, B, and C, respectively. By comparing the response results of Bridge A to Bridge B, the effects of flexural damage on the Bridge responses during earthquakes are examined. It is noted that Bridge B experiences larger displacement and suffers greater damage as reflected by higher damage index values. However, the difference is not significant and in most cases it is less than 10% since Bridge has sufficient flexural strength. Effects of shear damage on bridge behavior are studied by comparing the earthquake responses of Bridge A to those of Bridge C. It is noted that Bridges with shear damage generally experience larger displacement and suffer greater damage than Bridges with adequate shear capacity. The effects of shear damage on earthquake responses of older Bridges are more significant than those of flexural damage. From this example, it is important to consider the cumulated damage in seismic performance assessment of Bridges. By comparing the responses of Bridge B to Bridge C, the effects of shear degradation on Bridge responses are studied. Shear degradation in Bridge columns significantly increases seismic responses in Bridge C. It is noted in many cases, shear degradation in columns of Bridge C leads to the collapse of the Bridge as a result of insufficient shear capacity. Based on overview of all the results, it is found that shear degradation is an important factor that greatly impacts the response and behavior of old Bridges (Bridge C). The results show that consideration of flexural and shear degradation effects is necessary for the evaluation of the seismic performance of old Bridges. The proposed model is capable to more realistically predict the location, extent of damage and the cause of collapse in bridges. Figures 4e and 4f show the results of the global damage index of the example bridges. The global damage index also increases from Bridge A to Bridge C, which again signifies Bridge C suffers the most damage.

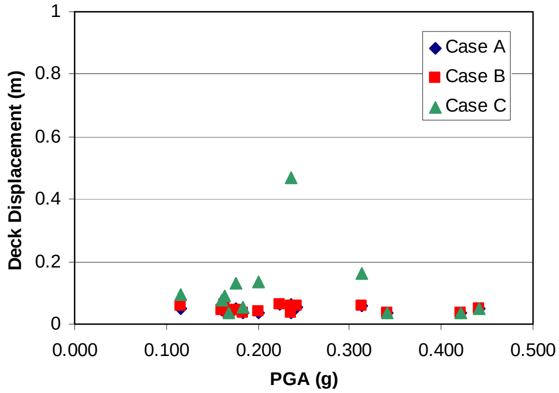

(a) Deck Displacement

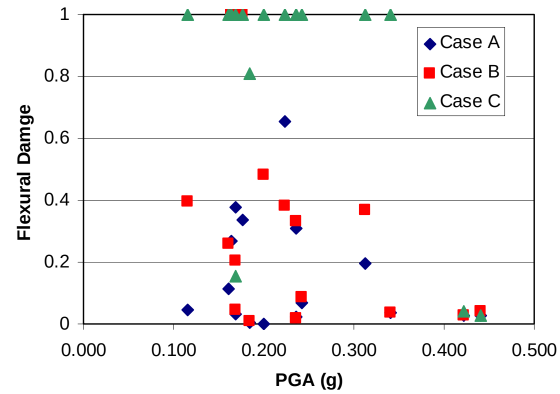

(b) Flexural Damage Index

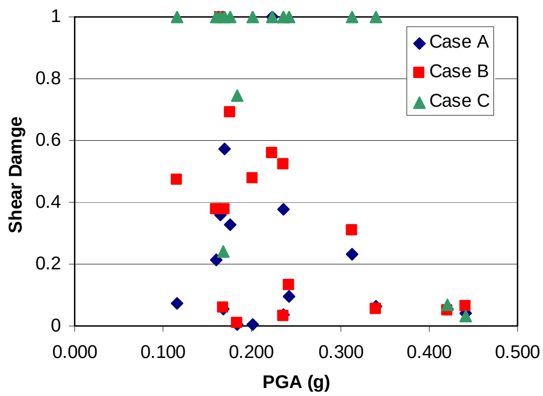

(c) Shear Damage Index

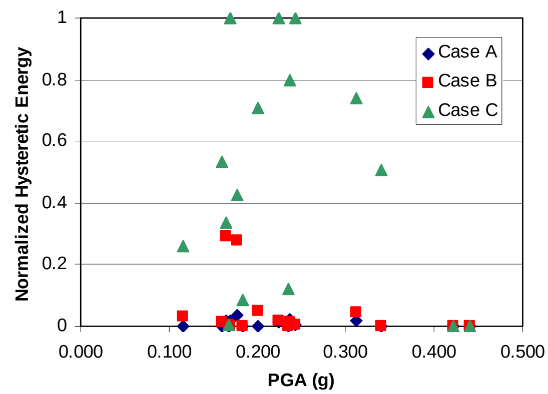

(d) Normalized Hysteretic Energy

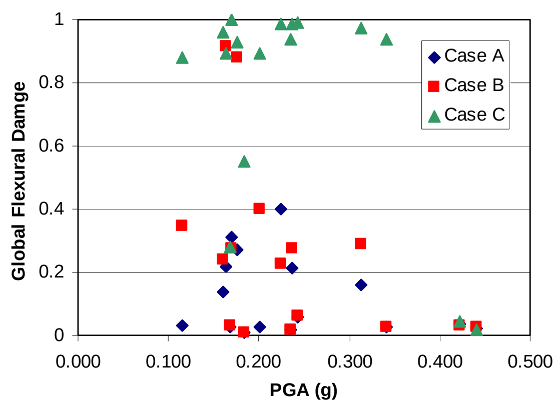

(e) Global Flexural Damage Index

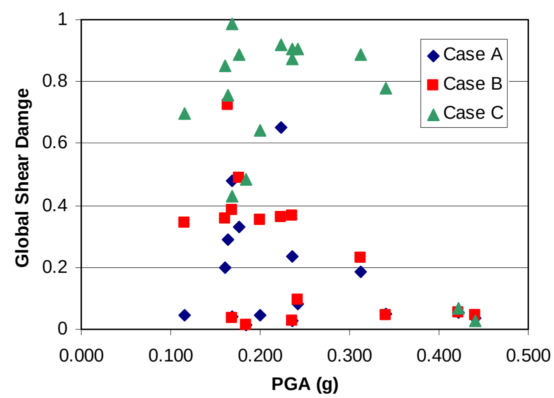

(f) Global Shear Damage Index

Figure 4 Comparison of Seismic Reponses.

4. CONCLUSIONS

This paper presented a three-dimensional nonlinear degrading stiffness model for the use in nonlinear earthquake response analyses of reinforced concrete bridges. The model can capture bilateral stiffness degradation behavior due to both flexural and shear damage. The stiffness matrix is derived from the assumption that the degradation is proportional to the degree of damage at element ends. Damage progresses from an undamaged state, which corresponds to a fixed-end condition to a complete flexural damage state, which corresponds to a pinned-end condition and to a complete shear and flexural damage state corresponds to a roller-end condition. The degrading stiffness matrix is computed by subtracting the products of the release stiffness matrices and the corresponding damage indices from the initial elastic stiffness. The modified Park and Ang's damage model is used to compute the flexural damage. To quantify the degree of shear damage in a reinforced concrete member a shear damage index is developed, which is based on the shear strength and shear demand relationship. Nonlinear earthquake response analyses of a three-span reinforced concrete bridge subjected to bi-directional strong earthquake ground motions have been carried out. It is concluded that by including the flexural degradation behavior in to the analytical model has increased the seismic demands on the bridges. For older bridges with inadequate shear capacity, the use of shear damage model is critical. The effects resulted from shear damage on the behavior of the bridge are more significant than those effects resulted from flexural damage. By considering flexural and shear damage, different nonlinear behavior and damage distribution patterns of the bridge are observed. With the consideration of shear degradation effects, the seismic vulnerability of typical old bridges designed prior to 1970s is demonstrated. The model can be used to accurately evaluate the seismic demands and the post-yield damage behavior of different types of bridge structures and is an important tool for archiving the objective of the performance-based design of bridges.

REFERENCES

Kunnath, S. K., Reinhorn, A. M. and Lobo, R. F. (1992). IDARC Version 3.0: A program for the inelastic damage analysis of reinforced concrete structures, Report No. NCEER-92-0022, National Center for Earthquake Engineering Research, State University of New York at Buffalo.

Park, Y. J. and Ang, H-S. (1985). Mechanistic seismic damage model for reinforced concrete, *Journal of Structural Engineering*, **111:4**, 722-739.

PEER strong motion database (2006). http://peer.berkeley.edu/smcat/ (accessed 5/1/2006).

Phung, V. (2005). Strong ground motions for bridge design and nonlinear dynamic response analysis of bridges, Ph.D. dissertation, Department of Civil and Environmental Engineering, Carleton University, Ottawa, Canada.

Priestley, M.J., Verma, R. and Xiao, Y. (1994). Seismic shear strength of reinforced concrete columns, *Journal of Structural Engineering*, **120:8**, 2310-2329.

Takeda, T., Sozen, M.A. and Neilsen N.N. (1970). Reinforced concrete response to simulated earthquake, *ACI Journal of Structural Division*, **96(ST12)**, 2557-2573.

Tseng, W.S. and Penzien, J. (1973). Analytical investigations of the seismic response of long multiple span highway bridges, UCB/EERC-73/12, Earthquake Engineering Research Center, University of California, Berkeley, CA.

Williams, M. S. and Sexsmith, R.G. (1995). Seismic damage indices for concrete structures: a state-of-the-art review, *Earthquake Spectra*, **11:2**, 319-349.

Wong, Y.L., Paulay, T. and Priestley, M.J.N. (1993). Response of circular reinforced concrete columns to multi-directional seismic attack, *ACI Struct. J.*, **90:2**, 180-191.

Zhang, Y., Cofer, W. F. and Mclean D. I. (1999). Analytical evaluation of retrofit strategies for multi-column bridges, *Journal of Bridge Engineering*, **4:2**, 143-150.